

Gradient-Based Speech-to-Text Alignment for Any ASR Model: From CTC to Speech LLMs

Albert Zeyer , Ralf Schlüter , Hermann Ney

Machine Learning and Human Language Technology Group, RWTH Aachen University, Aachen, Germany

AppTek GmbH, Aachen, Germany

{zeayer,schlueter,ney}@ml.rwth-aachen.de

Abstract—Speech-to-text alignment means finding the temporal boundaries of each word in the audio. Some models provide such an alignment directly and others do not. Connectionist temporal classification (CTC) and transducer models have an alignment by construction, whereas attention-based encoder-decoders (AED) and speech large language models (LLMs) do not, and their word timings are usually read off the attention weights instead. All of these signals live on the encoder frame grid, which bounds their temporal precision. We study a generic *gradient-based alignment* that applies to any differentiable ASR model. We take the gradient of each teacher-forced token log probability with respect to the input, reduce it to a per-frame saliency, and decode the resulting matrix into word boundaries with a single dynamic-programming pass. The method needs no training, no model modification and no alignment heads, works across all model families including the speech LLMs, and aligns on the input grid rather than on the coarser encoder grid. We evaluate it on sixteen models from four families, on read (TIMIT) and spontaneous (Buckeye) speech, each against the model’s own native or attention-based alignment. We find that the gradient yields a usable alignment for every model, that it is usually somewhat behind a strong native aligner but better where the native alignment is weak, as for the streaming models, and that its main disadvantage is the cost of one backward pass per token.

Index Terms—speech-to-text alignment, forced alignment, gradient-based attribution, automatic speech recognition, speech language models

I. INTRODUCTION & RELATED WORK

Speech-to-text alignment assigns each transcribed word a start and end time in the audio. It is classically produced by finding the best path through a Gaussian-mixture hidden Markov model (GM-HMM) which is still the most accurate aligner for read speech [1]–[5]. Current models, however, differ in what alignment they provide on their own [6]: connectionist temporal classification (CTC) [4], [7] and transducer models [8] have one by construction, whereas attention-based encoder-decoders (AED) [9]–[11] and speech large language models (LLMs) [12]–[14] do not, and their word timings are usually read off the attention weights instead. All of these signals live on the 20 to 80 ms encoder frame grid, which bounds their temporal precision. For AED, reading the timing off the cross-attention is established practice: Whisper emits coarse segment-level timestamp tokens [15], word-level timestamps follow from a dynamic time warping (DTW) of the decoder cross-attention [16] that fine-tuning can sharpen [17], and the alignment-bearing heads can even be selected by

an unsupervised heuristic and refined with character-level teacher forcing without any training [18]. Speech LLM self-attention carries a similar alignment, used to constrain text-to-speech synthesis [19] and as a policy for simultaneous translation [20]; forced alignment has separately been cast as a trained LLM task [21].

We study a generic *gradient-based alignment* that applies to any differentiable speech recognition model. For each transcript token we take the gradient of its teacher-forced log probability with respect to the input, reduce it to a per-frame saliency [22], and decode the resulting token-by-frame matrix into word boundaries with a single dynamic-programming pass (Fig. 1). As it uses the gradient w.r.t. the input signal, it aligns on the input grid rather than on the coarser encoder grid, and it can correct temporal shifts of the encoder: the encoder is often so powerful that it can displace the signal in time (e.g. with streaming models) or even reverse the time dimension [23]¹, which degrades the native forced alignment, while the gradient should still give a meaningful alignment. It needs no training and no model modification and it applies to all model families. Unlike the attention-based alignment, which first has to find which attention head carries the alignment (hand-picked for Whisper, and unpublished for the other models, so that we have to select it on a labeled development set), the gradient uses one canonical signal, the saliency of the token’s own log probability. In prior work, the same method has been applied to speech recognition AED models [18], [23] and machine-translation models [24].

This work is not a proposal of gradient alignment as the best aligner. A strong native aligner is usually still somewhat better, and the gradient is considerably more expensive. We rather provide a broad and fair analysis of what the gradient alignment is, how well it works across all the model families, and where it wins and loses. Our contributions are:

- We show that the gradient-based alignment applies to all ASR model families: CTC (prefix scores), transducers (RNN-T and TDT, also via prefix scores), AED, and speech LLMs.
- Improved alignment path scoring, where the best alignment path is found via dynamic programming. The cross-attention dynamic time warping (DTW) used by Whisper and CrisperWhisper is a special case of it. Our version

¹Arguably reversing the time dimension will not happen for CTC, though.

improves on that DTW both on the attention and on the gradient signal.

- For the speech LLMs, we read the alignment off their self-attention, the analog of the encoder-decoder cross-attention.
- A comprehensive and fair comparison of sixteen models across the four families, on read (TIMIT) and spontaneous (Buckeye) speech, each against its own native or attention-based alignment, including the tokenization granularity, the input-grid resolution, the recognition-mode alignment, and the compute cost.
- Public source code to reproduce all results including the whole pipeline.

II. ALIGNMENTS VIA GRADIENTS

We can calculate the gradient of the log probability $p(a_s | a_1^{s-1}, x_1^{T'})$ of some target label $a_s \in \mathcal{A}$ (the label vocabulary) in label position s , given the input $x_1^{T'}$ and the history $a_1^{s-1} \in \mathcal{A}^{s-1}$ of previous labels, w.r.t. an input frame x_t . The transcript a_1^S has S labels and the input T' frames; the saliency matrix and the alignment below have T time frames: $T = T'$ when the gradient is taken at the input, or the number of encoder frames when it is taken at an encoder layer. Comparing the norm of these gradients over the time frames t will give us an indication of the importance of each frame for this specific output label a_s . Specifically, we calculate the log norm²

$$G_{s,t} := \log \left\| \nabla_{x_t} \log p(a_s | a_1^{s-1}, x_1^{T'}) \right\|_p \in \mathbb{R}. \quad (1)$$

The matrix $\log \text{softmax}_T G$ in Fig. 1 shows the alignment clearly.

Note that $\log p(a_s | a_1^{s-1}, x_1^{T'})$ is straightforward to compute for an AED model or speech LLM (we exclude the EOS label here), and was done in a similar way in [18], [23]. It is possible for CTC and transducer as well, using the prefix scores [25] which can be calculated efficiently using dynamic programming.

To use this to get some alignment, we need to define which alignment label topology we allow (mapping a_1^S to y_1^T) and how to score one particular alignment y_1^T such that we can search for the one with the highest score.

For the label topology, we map a_1^S to y_1^T over $\mathcal{Y} = \mathcal{A} \cup \{\epsilon\}$, letting each real label repeat over consecutive frames with ϵ (blank/silence) labels in between. We write this as a finite state automaton with enumerated states $Y_1^{2S+1} = (\epsilon, 1, \epsilon, 2, \dots, S, \epsilon)$, whose $S+1$ blank states sit before the first label, between adjacent labels, and after the last. A topology is fixed by which of these blank states it permits, the rest being disallowed. Our default is a *word-level* topology: a blank only at word boundaries (before the first word, after the last, and between adjacent words), forbidding blanks inside a word, as we evaluate word boundaries. The *full*, CTC-like topology instead permits every blank (unlike CTC, we do not force a

²We found that the log norm was better conditioned than the norm, and yielded better results. We also tested different p -norms, and found $p = 2$ in most cases to perform best.

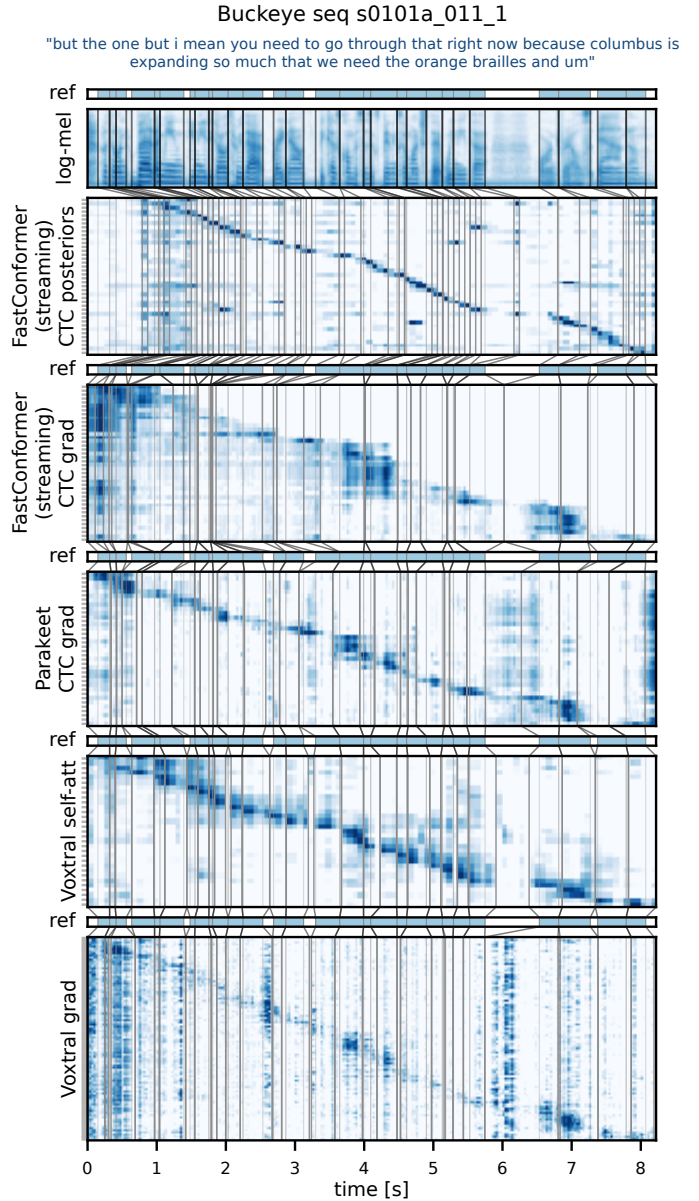


Fig. 1: Posteriors $\log \left(p_t(y=a_s | x_1^{T'}) \right)_{s,t} \in \mathbb{R}^{S \times T}$, gradient scores $\log \text{softmax}_T(G) \in \mathbb{R}^{S \times T}$, and log self-attention weights (in $\mathbb{R}^{S \times T}$), all without energy weighting here, each with word boundaries, in comparison to the reference segmentation (silence in white, words in blue, with word boundaries).

ϵ between two equal labels $a_s = a_{s+1}$), and a variant with *no interior silence* keeps only the leading and trailing blank, so adjacent tokens follow each other directly. We decode all topologies with the standard time-synchronous Viterbi search (as in CTC), advancing one frame per step, so every token spans at least one frame. Whisper and CrisperWhisper instead align the cross-attention by DTW, which additionally allows vertical transitions (advancing the token within a frame), so adjacent tokens may overlap by up to one frame; with no inte-

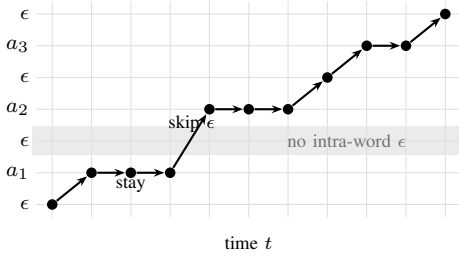


Fig. 2: Decoding the saliency into an alignment, for two words $(a_1 a_2)(a_3)$. The DP runs a time-synchronous Viterbi over the FSA states Y_1^{2S+1} (rows): per frame it stays, advances one state (+1), or skips a blank. The word-level topology shades out the intra-word blank (between a_1 and a_2), forcing a skip there, while keeping the word-boundary blank (state 5). DTW instead allows a vertical move (advancing the token within a frame), so adjacent tokens may overlap by up to one frame.

rior silence and without the log of eq. (3), our decoder reduces to that DTW up to those vertical transitions (Table VIII). We search for an allowed state sequence r_1^T , $r_t \in \{1, \dots, 2S+1\}$, compatible with a_1^S , that maximizes

$$\text{GradScore}(r_1^T) = \sum_{t=1}^T \begin{cases} G'_{Y_{r_t}, t}, & Y_{r_t} \neq \epsilon, \\ \beta_t, & Y_{r_t} = \epsilon, \end{cases} \quad (2)$$

with a token score G' and a silence score β_t defined below. The best r_1^T is found via dynamic programming (Fig. 2), and the alignment y_1^T read off with $y_t = a_{Y_{r_t}}$ for non-blank states and $y_t = \epsilon$ otherwise.

The token score is the over-time log-softmax of the (optionally energy-weighted) saliency,

$$G'_{s,t} = \log \text{softmax}_T(G + \rho \log E)_{s,t}, \quad (3)$$

where $\rho \geq 0$ is a weighting ($\rho = 0.5$ by default; $\rho = 0$ disables it) and $E_t \in [0, 1]$ a smoothed audio-energy envelope on the frame grid: from the waveform x we form the windowed root-mean-square energy $\tilde{E} = \sqrt{w * x^2}$, with w a normalized 25 ms Hann window ($\sum_i w_i = 1$) and $*$ convolution, sample it at the frame centers c_t , and normalize by its maximum, $E_t = \tilde{E}_{c_t} / \max_{c_t'} \tilde{E}_{c_t'}$. The energy weight suppresses the gradient's spurious response in silent frames.

The silence score β_t admits the constant blank of CTC, but also a self-calibrating blank derived from the per-frame statistics of the token scores. Let μ_t and σ_t be the mean and standard deviation of $\{G'_{s,t}\}_s$ over the labels s (taken at $\rho = 0$, so the blank calibrates against the raw saliency). We consider

$$\beta_t = \begin{cases} \gamma, & \text{(constant)} \\ \mu_t + \kappa \sigma_t, & \text{(z-score)} \\ \mu_t - \lambda z(E_t) \sigma_t, & \text{(energy)} \end{cases} \quad (4)$$

with $z(E_t) = (E_t - \bar{E}) / \text{std}(E)$ the z-score of the energy over the T frames (\bar{E} and $\text{std}(E)$ its mean and standard deviation), and hyperparameters γ (constant level), κ and λ . The energy blank is a VAD-style silence emission: in a low-energy frame

TABLE I: **Word-boundary error and accuracy per model**, gradient alignment vs. each model's native or attention aligner, on TIMIT-test and Buckeye, grouped by family. The attention and posterior aligners use the model's native subword units; the gradient uses characters for AED and speech-LLM and native subwords otherwise (Table IV). Starred Whisper-large-v3 gradient row (*) is taken at optimal encoder depth (encoder 3/4, Table X).

Type	Model Name	Align method	TIMIT		Buckeye	
			WBE [ms] ↓	≤50ms [%] ↑	WBE [ms] ↓	≤50ms [%] ↑
GM-HMM	MFA	Likelihood	19	92.3	32	90.0
CTC	MMS-FA	Gradients	49	64.3	121	58.2
		Posteriors	37	71.5	46	69.9
	XLS-R (Phoneme)	Gradients	49	65.7	81	66.4
		Posteriors	30	80.7	44	70.4
	Parakeet	Gradients	94	40.8	117	37.1
	CTC	Posteriors	77	39.4	99	32.2
	OWSM-CTC	Gradients	142	28.4	145	30.4
		Posteriors	120	20.6	110	25.2
FastConformer (streaming)	Gradients	127	32.0	158	30.1	
	Posteriors	357	1.1	366	2.2	
Transd.	Parakeet	Gradients	125	31.5	147	29.1
	RNN-T	Posteriors	79	39.3	93	35.4
	Parakeet	Gradients	128	32.9	157	27.5
	TDT	Posteriors	80	41.2	90	38.6
	Emformer (streaming)	Gradients	159	24.8	139	30.4
		Posteriors	394	0.3	399	0.5
FastConformer (streaming)	Gradients	153	27.3	189	24.0	
	Posteriors	307	3.6	331	3.9	
AED	Whisper-base	Gradients	51	59.3	75	52.7
		Cross-att.	51	62.3	62	66.3
	Whisper-large-v3	Gradients	55	57.8	53	66.2
		Gradients*	33	76.9	39	80.0
		Cross-att.	42	66.7	49	69.1
	Crisper-Whisper	Gradients	60	54.3	59	59.2
		Cross-att.	33	80.7	47	80.1
	OWLS-1B	Gradients	153	31.7	180	32.9
Cross-att.		35	76.7	51	69.1	
Speech LLM	Voxtral	Gradients	77	45.6	74	51.0
		Self-att.	53	61.1	52	65.5
	Phi-4-MM	Gradients	84	43.0	104	43.1
		Self-att.	68	46.6	79	39.8
	Canary-Qwen	Gradients	90	40.6	99	40.6
		Self-att.	131	28.0	211	16.3

$z(E_t) < 0$ raises β_t above the token mean, so the frame goes to the blank; in speech frames β_t drops below the token scores.

III. EXPERIMENTAL SETUP

We evaluate sixteen models from the four families. For reference we run two dedicated aligners, a GM-HMM via MFA [3], and MMS-FA [26], [27], a wav2vec 2.0 [28] CTC model built specifically for forced alignment. For CTC we further use XLS-R on phonemes [29], [30], Parakeet CTC [31], OWSM-CTC [32], [33], and a streaming FastConformer-CTC [34]. For the transducers we use Parakeet RNN-T [31] and TDT [35], and the streaming FastConformer-RNN-T [34] and Emformer [36], [37]. The AED models are Whisper base and large-v3 [15], CrisperWhisper [17], and OWLS-1B [38], and the speech LLMs are Voxtral [39], Phi-4-multimodal (Phi-4-MM) [40], and Canary-Qwen [41]. We align on TIMIT

TABLE II: **Hypothesis-mode alignment** on Buckeye, where each model aligns its own recognition. Identity-gated F1 at a 50 ms collar and Levenshtein-matched WBE against the reference.

Model		Ref-match [%]↑	WER [%]↓	Align method	Matched-WBE [ms]↓	F1 ≤50ms [%]↑
Type	Name					
CTC	Parakeet CTC	92.3	11.9	Gradients	116	14.0
				Posteriors	99	11.1
	OWSM-CTC	89.2	14.3	Gradients	142	9.9
				Posteriors	114	5.4
FastConformer (streaming)	86.5	16.8	Gradients	164	9.7	
			Posteriors	363	0.2	
Transd.	Parakeet RNN-T	89.8	13.6	Gradients	156	7.6
				Posteriors	92	13.2
	Parakeet TDT	91.8	12.8	Gradients	155	7.8
				Posteriors	86	17.1
	Emformer (streaming)	72.1	30.5	Gradients	155	7.1
				Posteriors	391	0.0
	FastConformer (streaming)	87.1	15.9	Gradients	206	5.9
				Posteriors	318	0.4
AED	Whisper-base	85.5	18.0	Gradients	85	25.5
				Cross-att.	77	35.8
	Whisper-large-v3	88.1	15.3	Gradients	66	40.4
				Cross-att.	66	40.4
	Crisper-Whisper	92.0	12.7	Gradients	56	33.8
				Cross-att.	44	59.6
		92.6	12.2	Official	46	43.5
				Gradients	1024	3.8
OWLS-1B	85.7	208.0	Cross-att.	1312	7.8	
			Gradients	87	25.3	
Speech LLM	Voxtral	88.3	15.3	Self-att.	67	37.4
				Gradients	102	19.0
	Phi-4-MM	92.8	11.7	Self-att.	80	16.0
				Gradients	95	17.1
	Canary-Qwen	93.1	11.4	Self-att.	212	3.9
				Gradients	95	17.1

(test) [42] and on Buckeye spontaneous speech [43], both with gold word boundaries. For Buckeye we use a 5 h subset stratified by speaker (all speakers represented proportionally), split at every ≥ 1 s inter-word silence, then split any piece still longer than 18 s at its largest internal gap³. We report the word-boundary error (WBE), i.e. the mean per-word start and end absolute error, averaged over all words in the corpus⁴, and the accuracy at a collar, i.e. the fraction of all boundaries within 50 ms over the corpus. We compare each model against its own alignment, i.e. the CTC or transducer forced alignment on the model’s own emission (the “posteriors”), the AED cross-attention DTW [16], and, for the speech LLMs, the analogous text-to-audio self-attention, decoded by the same dynamic program as the gradient scores. We select the attention heads by per-head WBE on TIMIT development gold and average the top 8 heads. In hypothesis mode, where the recognition differs from the reference, we match the words by identity and report an identity-gated F1 at a 50 ms collar together with the matched WBE.

IV. RESULTS

a) *Alignment quality across model families:* Table I compares the gradient alignment versus each model’s own

³ [4] drops long utterances, but we keep them by splitting.

⁴ [5] averages first per utterance and then over utterances.

TABLE III: **Signed boundary offsets** on Buckeye, gradient alignment vs. the model’s alternative aligner. WBE is the mean absolute word-boundary error, start/end off. the signed mean boundary offset (positive = late), and width err. the signed word-width error (0 = correct duration). Parakeet RNN-T is the offline contrast to the streaming transducers.

Model		Align method	WBE [ms]↓	Start off. [ms]	End off. [ms]	Width err. [ms]
Type	Name					
CTC	MMS-FA	Gradients	121	-93	-91	+2
		Posteriors	46	+47	-14	-60
	XLS-R (Phoneme)	Gradients	81	-72	-47	+25
		Posteriors	44	+46	-14	-60
	Parakeet CTC	Gradients	117	-33	-54	-21
		Posteriors	99	+53	-51	-104
	OWSM-CTC	Gradients	145	-89	-107	-18
		Posteriors	110	+125	-10	-136
FastConformer (streaming)	Gradients	158	-62	-97	-35	
	Posteriors	366	+415	+310	-106	
Transd.	Parakeet RNN-T	Gradients	147	-22	-42	-20
		Posteriors	93	+42	-70	-113
	Emformer (streaming)	Gradients	139	+67	+32	-35
		Posteriors	399	+484	+308	-176
	FastConformer (streaming)	Gradients	189	-85	-123	-37
		Posteriors	331	+386	+260	-126
AED	Whisper-base	Gradients	75	+4	-4	-9
		Cross-att.	62	-38	-19	+19

TABLE IV: **Character vs. subword targets**, one representative model per family, Buckeye. Each model shows its gradient alignment and its model-native alternative. The character target is a valid re-segmentation of the transcript, one token per character with a word-boundary token between words.

Model		Align method	Char		Subword	
Type	Name		WBE [ms]↓	≤50ms [%]↑	WBE [ms]↓	≤50ms [%]↑
CTC	Parakeet CTC	Gradients	4167	2.8	117	37.1
		Posteriors	173	26.1	99	32.2
Transd.	Parakeet RNN-T	Gradients	384	22.1	147	29.1
		Posteriors	1255	14.8	93	35.4
AED	Whisper-large-v3	Gradients	53	66.2	108	41.2
		Cross-att.	57	75.2	49	69.1
Speech LLM	Voxtral	Gradients	74	51.0	118	38.0
		Self-att.	129	46.0	52	65.5

native or attention aligner, across CTC, AED, transducer and speech-LLM families. Gradient alignment is competitive on every family, beats the native alignment where it is weak (the streaming models, Canary-Qwen), and at the starred best encoder depth it also beats the Whisper-large-v3 cross-attention. The streaming posteriors’ large error is largely a systematic emission-delay bias rather than scatter (Table III and Fig. 1); the same table shows that gradient alignment shifts both boundaries together (a positional lead) rather than shrinking the word like the posteriors do.

Table II aligns each model’s own recognition (identity-gated F1 at a 50 ms collar and matched WBE), showing that gradient alignment remains usable when the hypothesis differs from the reference.

b) *Tokenization and the attention baseline:* Table IV justifies the tokenization we use throughout: the gradient alignment uses character targets for the AED and speech-

TABLE V: **Grad-score ablation** across families, Buckeye. The feature-axis reduction (L0.5 / L1 / L2 / sum), and whether the gradient is multiplied by the input (the right group). The signed sum columns need special handling, since their score can be negative: normalized score, constant blank score, on plain CTC topology.

Model		WBE [ms] ↓					
Type	Name	∇ (gradient)				∇ × input	
		L0.5	L1	L2	sum	L2	sum
CTC	MMS-FA	121	121	121	197	120	164
	Parakeet CTC	118	117	117	172	116	166
Transd.	Parakeet RNN-T	147	147	147	181	146	188
	Emformer (streaming)	142	140	139	184	138	190
AED	Whisper-base	74	74	75	110	76	122
	Voxtral	73	74	74	112	76	121
Speech LLM	Phi-4-MM	107	106	104	138	103	119
	Canary-Qwen	100	100	99	107	99	113

TABLE VI: **Blank-scoring scheme** across signals, Buckeye, word-level topology, energy weighting fixed at $\rho=0.5$. The constant blank γ , the energy-aware silence $\beta_t = \mu_t - \lambda z(E_t) \sigma_t$, and the z-score $\beta_t = \mu_t + \kappa \sigma_t$. WBE for the gradient signal and for the native attention signal.

Blank	Opts	WBE [ms] ↓						
		Gradients			Cross-att.		Self-att.	
		MMS-FA	Whisper	OWLS	Voxtral	Whisper	OWLS	Voxtral
constant	$\gamma = -3$	176	129	658	183	100	74	63
	$\gamma = -5$	131	87	577	131	44	65	53
	$\gamma = -8$	141	65	237	94	65	70	65
energy	$\lambda = 0.5$	131	54	193	77	63	65	59
	$\lambda = 1$	127	53	188	75	61	60	56
	$\lambda = 2$	121	53	180	74	49	51	52
	$\lambda = 3$	117	54	174	75	48	48	55
z-score	$\kappa = 0.5$	130	54	192	77	63	65	59
	$\kappa = 1$	127	53	186	75	61	59	56
	$\kappa = 2$	123	56	181	78	54	51	60

LLM families and subword targets for CTC and transducers, while every attention or posterior baseline uses the model’s native subword tokens. Character targets improve the gradient markedly for the autoregressive families (on Whisper-large-v3 and Voxtral the char gradient is well below the subword gradient), but they do not help the model-native attention aligners, and for the non-autoregressive CTC and transducer, which have no per-character acoustic emission, char-level collapses: char targets are consistently worse than subword for both the gradient and the posteriors, in the worst cases by an order of magnitude.

c) *Ablations*: The grad. score per-token reduction (Table V) moves WBE by only a few ms across the p -norms, while the plain sum is clearly worse, and gradient versus gradient- \times -input [44], [45] is within ~ 1 – 3 ms with neither winning consistently. Multi-pass attribution (SmoothGrad [46], VarGrad [47], Integrated [48] and Expected Gradients [49]) does not beat the single-pass gradient (numbers omitted here). Most decoding options behave consistently (Tables VI to VIII): the gradient is active even in silence and needs the energy-aware ($\lambda \approx 2$) or z-score blank, whereas the attention is

TABLE VII: **Audio-energy token weighting**, Buckeye, word-level topology. The token scores are weighted by (audio energy) $^\rho$ before the DP, and we sweep ρ ($\rho=0$ disables it) at each blank scheme. This complements Table VI, which sweeps the blank scheme at fixed $\rho=0.5$.

Blank	ρ	WBE [ms] ↓						
		Gradients			Cross-att.		Self-att.	
		MMS-FA	Whisper	OWLS	Voxtral	Whisper	OWLS	Voxtral
constant $\gamma = -5$	0.0	147	99	884	174	54	77	59
	0.25	140	89	700	141	48	71	56
	0.5	131	87	577	131	44	65	53
	0.75	126	89	512	131	45	60	52
	1.0	124	92	485	137	47	57	52
energy $\lambda = 1$	0.0	141	70	263	94	64	67	62
	0.25	136	58	212	81	63	65	59
	0.5	127	53	188	75	61	60	56
	0.75	119	53	177	75	57	57	54
	1.0	116	56	171	77	52	53	53
z-score $\kappa = 1$	0.0	142	70	263	94	65	66	64
	0.25	137	57	210	81	63	64	59
	0.5	127	53	186	75	61	59	56
	0.75	120	54	175	76	57	55	54
	1.0	117	57	173	79	52	52	54

TABLE VIII: **Whisper’s cross-attention DTW vs. our aligner** (Whisper-base cross-attention or grad. scores, Buckeye). Top row reproduces Whisper’s `find_alignment`. Columns: alignment-head set (Whisper’s curated heads, our gold-tuned top- k , or single best), token z-norm, median filter, pre-log of the score matrix (\log), log-softmax over time ($\log sm$; DP sums these log-scores), mono (\checkmark = our monotonic DP forbidding vertical step; \times = Whisper DTW), silence topology ($word$ = blank only between words; $none$ = no blank), and energy weighting (en).

Configuration	heads	z-norm	med. filt.	log	log sm	mono	sil.	en.	WBE [ms] ↓	
Cross-attn										
Whisper (faithful)	Whisper	\checkmark	\checkmark	\times	\times	\checkmark	none	\times	85	
+ energy									\checkmark	89
+ mono DP										84
+ silence										84
+ no median-filter									\times	85
+ no z-norm										83
+ log softmax										81
+ mono DP										83
+ silence										76
+ our heads									ours	
+ single best head	1-best	\checkmark		\times	\times		none		95	
ours (full)	ours	\times	\times	\checkmark	\checkmark	\checkmark	word	\checkmark	71	
+ DTW									73	
+ no energy									\times	71
+ no silence									\checkmark	117
Grad										
ours (full)	-	-	-	\checkmark	\checkmark	\times	word	\checkmark	75	
+ DTW, word-topo									76	
+ no word-topo									138	
+ no energy									\times	152

already silence-aware and a constant blank suffices; the z-score blank is the energy-free option that matches the energy one for gradients. The audio-energy token-weighting exponent matters little around our default and behaves consistently across the blank schemes (Table VII). For the cross-attention DTW, the dominant gain over the original Whisper heuristic is the gold-

TABLE IX: **MMS-FA (wav2vec 2.0) CTC gradient alignment across the internal level the gradient is taken at**, Buckeye. The levels run from the convolutional feature encoder through the feature projection to the raw waveform at several pooling rates. The feat-proj linear row equals the MMS-FA gradient number reported in Table I.

Gradient w.r.t.	ms/frame	Grid [Hz]	WBE [ms] ↓	≤50ms [%] ↑
Conv 0	0.31	3200	137	48.7
Conv 1	0.62	1600	133	49.5
Conv 2	1.25	800	133	49.5
Conv 3	2.5	400	132	50.0
Conv 4	5	200	130	50.8
Conv 5	10	100	128	52.3
Feat-proj LayerNorm	20	50	122	55.3
Feat-proj Linear	20	50	121	58.2
Raw waveform, pool 320	20	50	135	52.1
Raw waveform, pool 80	5	200	140	48.4
Raw waveform, pool 16	1	1000	142	47.5
Raw waveform, pool 1	0.0625	16000	134	47.7

TABLE X: **Encoder depth the gradient is taken at** for gradient alignment. Buckeye. Rows run from log-mel input through encoder to its output. Whisper-large-v3 uses char targets (32 layers; 1/4 etc. = L8/16/24) and FastConformer-CTC subword targets (17 layers; L4/9/13). Off. is mean signed boundary offset (positive = late).

Gradient w.r.t.	Whisper-large-v3 (char)				FastConformer-CTC			
	Grid [Hz]	WBE [ms] ↓	≤50ms [%] ↑	Off. [ms]	Grid [Hz]	WBE [ms] ↓	≤50ms [%] ↑	Off. [ms]
Log-mel in	100	53	66.2	-10	100	158	30.1	-80
Encoder in		44	74.6	-9		152	30.0	-63
Encoder 1/4		42	76.3	-9		145	29.4	-33
Encoder 1/2	50	41	78.2	-9	12.5	146	23.9	+73
Encoder 3/4		39	80.0	-9		229	12.5	+196
Encoder out		42	79.0	-13		305	4.9	+274

TABLE XI: **OWSM-CTC alignment from each inter-CTC block** (6/12/15/21) and the final block (27). Gradient alignment vs. posterior alignment.

Emit block	WBE [ms] ↓			
	TIMIT		Buckeye	
	Grad.	Post.	Grad.	Post.
6	142	120	145	110
12	150	124	167	118
15	160	125	183	119
21	168	125	194	120
27 (final)	172	125	198	121

tuned head selection (its curated set includes some near-useless heads); the Whisper-DTW setting is exactly our decoder with the log-compression and the blank state removed, and energy weighting helps the gradient but not the cross-attention DTW.

d) Where the gradient is taken: For MMS-FA, which is a wav2vec 2.0 model [28] (Table IX), the gradient localizes best at the feature-projection output (20 ms encoder grid); finer levels (the convolutional feature encoder, or the raw waveform pooled down to sample resolution) do not help, and the raw-waveform gradient is noisier. Table X sweeps the depth for Whisper-large-v3 and the FastConformer-CTC, from the log-

TABLE XII: **Cost of gradient alignment**, single GPU, subset of TIMIT, as real-time factor (RTF) $\times 10^3$ (ms compute per second of audio). Stages: Forward (encoder \rightarrow logits, shared with native methods), prefix-sum (CTC/transducer only), and backward (encoder VJP, batched). Grad. align extra cost is prefix-sum + backward; Shared DP align is excluded.

Model		Compute time [RTF $\times 10^3$]			
Type	Name	Model		Prefix-sum	
		Fwd	Bwd	Fwd	Bwd
CTC	MMS-FA	6	57	3	212
AED	Whisper-large-v3	24	277		
Speech LLM	Phi-4-MM	26	216		n/a

mel input through the encoder to its output (the activation just before the decoder / CTC linear): the sharpest gradient is at an intermediate depth (three quarters of the Whisper encoder, the L24 of the starred row in Table I; a quarter for the FastConformer-CTC), not the input, and in the streaming FastConformer-CTC the encoder’s time shift accumulates with depth, so its output gradient ends as delayed as its posteriors (Fig. 1).

e) Speech-LLM prompt influence: Gradient alignment is robust to the prompt used across all the speech LLMs and across the gradient-vs-self-attention signal (numbers omitted).

f) Inter-CTC: OWSM-CTC has intermediate CTC losses [32], [33], which we can use to take the gradient at each block of the encoder (Table XI). Interestingly, the earlier blocks are better than the later ones, both for the gradient and for the native CTC alignment.

g) Time stretch: Under audio time-stretch (numbers omitted), the same upsampling mechanism acts with opposite sign: it hurts a fine-grid model (MMS-FA) but helps a coarse-grid one (Voxtral) at mild factors.

h) Compute cost: The only extra cost over the native methods is the per-token backward (Table XII); the forward and the DP decode are shared, and for the CTC the per-token prefix-score lattice backward dominates.

V. CONCLUSION

Gradient alignment produces a usable word alignment for every model and family we tried, including the speech LLMs that have no built-in word aligner. It is usually a little behind a strong native aligner, but clearly better where that alignment is weak, as on the streaming models and Canary-Qwen, and on Whisper-large-v3 it even beats its cross-attention at the best encoder depth. Our decoder also improves on Whisper’s cross-attention DTW itself (Table VIII). Its input-grid resolution lets finer character targets improve accuracy, which the coarse attention grid cannot exploit. The per-token backward makes it much more expensive than a single forward, so we do not propose it as a practical aligner. The result is rather that one training-free input saliency aligns every differentiable ASR model across all four families, in some cases even better than the model’s own alignment. Beyond alignment, the gradient also serves as an analysis tool.

ACKNOWLEDGMENT

This work was partially supported by NeuroSys, which as part of the initiative “Clusters4Future” is funded by the Federal Ministry of Research, Technology and Space BMFTR (funding IDs 03ZU2106DA and 03ZU2106DD), and by the project RESCALE within the program *AI Lighthouse Projects for the Environment, Climate, Nature and Resources* funded by the Federal Ministry for the Environment, Nature Conservation, Nuclear Safety and Consumer Protection (BMUV), funding ID: 67KI32006A. The authors gratefully acknowledge the computing time provided to them at the NHR Center NHR4CES at RWTH Aachen University (project number p0023999). This is funded by the Federal Ministry of Education and Research, and the state governments participating on the basis of the resolutions of the GWK for national high performance computing at universities (www.nhr-verein.de/unsere-partner).

AI-GENERATED CONTENT DISCLOSURE

We used AI assistants (large language models) substantially in this work, to help set up and run the experiments, to debug and write parts of the code, and to draft and edit parts of this paper. All results were verified by the authors, who take full responsibility for the content.

REFERENCES

- [1] M. Gales and S. Young, “The application of hidden Markov models in speech recognition,” *Found. Trends Signal Process.*, vol. 1, no. 3, pp. 195–304, Jan. 2008.
- [2] L. R. Rabiner, “A tutorial on hidden Markov models and selected applications in speech recognition,” *Proc. of the IEEE*, vol. 77, no. 2, pp. 257–286, 1989.
- [3] M. McAuliffe, M. Socolof, S. Mihuc, M. Wagner, and M. Sonderegger, “Montreal Forced Aligner: Trainable text-speech alignment using Kaldi,” in *Proc. Interspeech*, 2017, pp. 498–502.
- [4] R. Huang, X. Zhang, Z. Ni, L. Sun, M. Hira, J. Hwang, V. Manohar, V. Pratap, M. Wiesner, S. Watanabe, D. Povey, and S. Khudanpur, “Less peaky and more accurate CTC forced alignment by label priors,” in *Proc. IEEE ICASSP*, 2024, pp. 11 831–11 835.
- [5] R. Rousso, E. Cohen, J. Keshet, and E. Chodroff, “Tradition or innovation: A comparison of modern asr methods for forced alignment,” in *Proc. Interspeech*, 2024, pp. 1525–1529.
- [6] R. Prabhavalkar, T. Hori, T. N. Sainath, R. Schlüter, and S. Watanabe, “End-to-end speech recognition: A survey,” *IEEE/ACM Trans. Audio, Speech, and Language Processing*, vol. 32, pp. 325–351, 2023.
- [7] A. Graves, S. Fernández, F. Gomez, and J. Schmidhuber, “Connectionist temporal classification: labelling unsegmented sequence data with recurrent neural networks,” in *Proceedings of the 23rd international conference on Machine learning*. ACM, 2006, pp. 369–376.
- [8] A. Graves, “Sequence transduction with recurrent neural networks,” ArXiv:1211.3711, ICML Representation Learning Workshop, 2012.
- [9] J. K. Chorowski, D. Bahdanau, D. Serdyuk, K. Cho, and Y. Bengio, “Attention-based models for speech recognition,” in *NIPS*, 2015, pp. 577–585.
- [10] W. Chan, N. Jaitly, Q. V. Le, and O. Vinyals, “Listen, attend and spell: A neural network for large vocabulary conversational speech recognition,” in *Proc. IEEE ICASSP*, 2016, pp. 4960–4964.
- [11] A. Zeyer, K. Irie, R. Schlüter, and H. Ney, “Improved training of end-to-end attention models for speech recognition,” in *Interspeech*, Hyderabad, India, Sep. 2018.
- [12] D. Zhang, S. Li, X. Zhang, J. Zhan, P. Wang, Y. Zhou, and X. Qiu, “SpeechGPT: Empowering large language models with intrinsic cross-modal conversational abilities,” in *Findings of the Association for Computational Linguistics: EMNLP 2023*, H. Bouamor, J. Pino, and K. Bali, Eds. Singapore: Association for Computational Linguistics, Dec. 2023, pp. 15 757–15 773. [Online]. Available: <https://aclanthology.org/2023.findings-emnlp.1055/>
- [13] Y. Chu, J. Xu, X. Zhou, Q. Yang, S. Zhang, Z. Yan, C. Zhou, and J. Zhou, “Qwen-Audio: Advancing universal audio understanding via unified large-scale audio-language models,” ArXiv:2311.07919, 2023.
- [14] R. Schmitt, A. Zeyer, M. Zeineldeen, R. Schlüter, and H. Ney, “LLMs and speech: Integration vs. combination,” Arxiv:2603.15045, Mar. 2026. [Online]. Available: <https://arxiv.org/abs/2603.15045>
- [15] A. Radford, J. W. Kim, T. Xu, G. Brockman, C. Mcleavy, and I. Sutskever, “Robust speech recognition via large-scale weak supervision,” in *Proc. ICML*, ser. Proceedings of Machine Learning Research, A. Krause, E. Brunskill, K. Cho, B. Engelhardt, S. Sabato, and J. Scarlett, Eds., vol. 202. PMLR, 23–29 Jul 2023, pp. 28 492–28 518. [Online]. Available: <https://proceedings.mlr.press/v202/radford23a.html>
- [16] M. Bain, J. Huh, T. Han, and A. Zisserman, “WhisperX: Time-accurate speech transcription of long-form audio,” in *Proc. Interspeech*, 2023, pp. 4489–4493.
- [17] M. Zusag, L. Wagner, and B. Thallinger, “CrisperWhisper: Accurate timestamps on verbatim speech transcriptions,” in *Proc. Interspeech*, 2024, pp. 1265–1269.
- [18] S.-L. Yeh, Y. Meng, and H. Tang, “Whisper has an internal word aligner,” in *Proc. IEEE ASRU*, 2025.
- [19] H. Wang, C. Du, Y. Guo, S. Wang, X. Chen, and K. Yu, “Attention-constrained inference for robust decoder-only text-to-speech,” ArXiv 2404.19723, 2024. [Online]. Available: <https://arxiv.org/abs/2404.19723>
- [20] S. Papi and L. Bentivogli, “DOA: Training-free decoder-only attention policy for long-form simultaneous translation with SpeechLLMs,” ArXiv 2605.31432, 2026. [Online]. Available: <https://arxiv.org/abs/2605.31432>
- [21] B. Mu, X. Shi, X. Wang, H. Liu, J. Xu, and L. Xie, “LLM-ForcedAligner: A non-autoregressive and accurate llm-based forced aligner for multilingual and long-form speech,” ArXiv 2601.18220, 2026. [Online]. Available: <https://arxiv.org/abs/2601.18220>
- [22] K. Simonyan, A. Vedaldi, and A. Zisserman, “Deep inside convolutional networks: Visualising image classification models and saliency maps,” ArXiv:1312.6034; ICLR Workshop Track, 2014.
- [23] R. Schmitt, A. Zeyer, M. Zeineldeen, R. Schlüter, and H. Ney, “The conformer encoder may reverse the time dimension,” in *Proc. IEEE ICASSP*, Hyderabad, India, Apr. 2025, preprint ArXiv:2501.04521.
- [24] S. Ding, H. Xu, and P. Koehn, “Saliency-driven word alignment interpretation for neural machine translation,” in *Proceedings of the Fourth Conference on Machine Translation (Volume 1: Research Papers)*, O. Bojar, R. Chatterjee, C. Federmann, M. Fishel, Y. Graham, B. Haddow, M. Huck, A. J. Yepes, P. Koehn, A. Martins, C. Monz, M. Negri, A. Névöl, M. Neves, M. Post, M. Turchi, and K. Verspoor, Eds. Florence, Italy: Association for Computational Linguistics, Aug. 2019, pp. 1–12. [Online]. Available: <https://aclanthology.org/W19-5201/>
- [25] T. Hori, S. Watanabe, and J. Hershey, “Joint CTC/attention decoding for end-to-end speech recognition,” in *Proc. ACL*, R. Barzilay and M.-Y. Kan, Eds. Vancouver, Canada: Association for Computational Linguistics, Jul. 2017, pp. 518–529. [Online]. Available: <https://aclanthology.org/P17-1048>
- [26] V. Pratap, A. Tjandra, B. Shi, P. Tomasello, A. Babu, S. Kundu, A. Elkahky, Z. Ni, A. Vyas, M. Fazel-Zarandi, A. Baeviski, Y. Adi, X. Zhang, W.-N. Hsu, A. Conneau, and M. Auli, “Scaling speech technology to 1,000+ languages,” *Journal of Machine Learning Research*, vol. 25, no. 1, Jan. 2024.
- [27] J. Hwang, M. Hira, C. Chen, X. Zhang, Z. Ni, G. Sun, P. Ma, R. Huang, V. Pratap, Y. Zhang, A. Kumar, C.-Y. Yu, C. Zhu, C. Liu, J. Kahn, M. Ravanelli, P. Sun, S. Watanabe, Y. Shi, and Y. Tao, “TorchAudio 2.1: Advancing speech recognition, self-supervised learning, and audio processing components for PyTorch,” in *Proc. IEEE ASRU*, 2023, pp. 1–9.
- [28] A. Baeviski, Y. Zhou, A. Mohamed, and M. Auli, “wav2vec 2.0: A framework for self-supervised learning of speech representations,” in *Proc. NeurIPS*, H. Larochelle, M. Ranzato, R. Hadsell, M. Balcan, and H. Lin, Eds., vol. 33. Curran Associates, Inc., 2020, pp. 12 449–12 460. [Online]. Available: https://proceedings.neurips.cc/paper_files/paper/2020/file/92d1e1eb1cd6f9fba3227870bb6d7f07-Paper.pdf

- [29] V. Phy, "Automatic phoneme recognition on TIMIT dataset with Wav2Vec 2.0," 2022. [Online]. Available: <https://huggingface.co/vitoutophy/wav2vec2-xls-r-300m-timit-phoneme>
- [30] A. Babu, C. Wang, A. Tjandra, K. Lakhotia, Q. Xu, N. Goyal, K. Singh, P. von Platen, Y. Saraf, J. Pino, A. Baevski, A. Conneau, and M. Auli, "XLS-R: Self-supervised cross-lingual speech representation learning at scale," in *Proc. Interspeech*, 2022, pp. 2278–2282.
- [31] D. Rekish, N. R. Koluguri, S. Kriman, S. Majumdar, V. Noroozi, H. Huang, O. Hrinchuk, K. Puvvada, A. Kumar, J. Balam, and B. Ginsburg, "Fast conformer with linearly scalable attention for efficient speech recognition," in *Proc. IEEE ASRU*, 2023, pp. 1–8.
- [32] Y. Peng, S. Muhammad, Y. Sudo, W. Chen, J. Tian, C.-J. Lin, and S. Watanabe, "OWSM v4: Improving open whisper-style speech models via data scaling and cleaning," in *Proc. Interspeech*, 2025.
- [33] Y. Peng, Y. Sudo, M. Shakeel, and S. Watanabe, "OWSM-CTC: An open encoder-only speech foundation model for speech recognition, translation, and language identification," in *Proc. ACL*, 8 2024, pp. 10 192–10 209. [Online]. Available: <https://aclanthology.org/2024.acl-long.549>
- [34] V. Noroozi, S. Majumdar, A. Kumar, J. Balam, and B. Ginsburg, "Stateful conformer with cache-based inference for streaming automatic speech recognition," in *Proc. IEEE ICASSP*, 2024, pp. 12 041–12 045.
- [35] H. Xu, F. Jia, S. Majumdar, H. Huang, S. Watanabe, and B. Ginsburg, "Efficient sequence transduction by jointly predicting tokens and durations," in *Proc. ICML*, ser. Proceedings of Machine Learning Research, A. Krause, E. Brunskill, K. Cho, B. Engelhardt, S. Sabato, and J. Scarlett, Eds., vol. 202. PMLR, 23–29 Jul 2023, pp. 38 462–38 484. [Online]. Available: <https://proceedings.mlr.press/v202/xu23g.html>
- [36] Y. Shi, Y. Wang, C. Wu, C.-F. Yeh, J. Chan, F. Zhang, D. Le, and M. Seltzer, "Emformer: Efficient memory transformer based acoustic model for low latency streaming speech recognition," in *Proc. IEEE ICASSP*, 2021, pp. 6783–6787.
- [37] Y.-Y. Yang, M. Hira, Z. Ni, A. Astafurov, C. Chen, C. Puhrsch, D. Pollack, D. Genzel, D. Greenberg, E. Z. Yang, J. Lian, J. Hwang, J. Chen, P. Goldsborough, S. Narenthiran, S. Watanabe, S. Chintala, and V. Quenneville-Bélaïr, "TorchAudio: Building blocks for audio and speech processing," in *Proc. IEEE ICASSP*, 2022, pp. 6982–6986.
- [38] W. Chen, J. Tian, Y. Peng, B. Yan, C.-H. H. Yang, and S. Watanabe, "OWLS: Scaling laws for multilingual speech recognition and translation models," in *Proc. ICML*, 2025. [Online]. Available: <https://openreview.net/forum?id=xnPW7yYomF>
- [39] Mistral AI, "Voxtral," arXiv:2507.13264, 2025.
- [40] A. Abouelenin, A. Ashfaq, A. Atkinson, H. Awadalla, N. Bach, J. Bao, A. Benhaim, M. Cai, V. Chaudhary, C. Chen, D. Chen, D. Chen, J. Chen, W. Chen, Y.-C. Chen, Y. ling Chen, Q. Dai, X. Dai, R. Fan, M. Gao, M. Gao, A. Garg, A. Goswami, J. Hao, A. Hendy, Y. Hu, X. Jin, M. Khademi, D. Kim, Y. J. Kim, G. Lee, J. Li, Y. Li, C. Liang, X. Lin, Z. Lin, M. Liu, Y. Liu, G. Lopez, C. Luo, P. Madan, V. Mazalov, A. Mitra, A. Mousavi, A. Nguyen, J. Pan, D. Perez-Becker, J. Platin, T. Portet, K. Qiu, B. Ren, L. Ren, S. Roy, N. Shang, Y. Shen, S. Singhal, S. Som, X. Song, T. Sych, P. Vaddamanu, S. Wang, Y. Wang, Z. Wang, H. Wu, H. Xu, W. Xu, Y. Yang, Z. Yang, D. Yu, I. Zabir, J. Zhang, L. L. Zhang, Y. Zhang, and X. Zhou, "Phi-4-mini technical report: Compact yet powerful multimodal language models via mixture-of-loras," ArXiv 2503.01743, 2025. [Online]. Available: <https://arxiv.org/abs/2503.01743>
- [41] K. C. Puvvada, P. Żelasko, H. Huang, O. Hrinchuk, N. R. Koluguri, K. Dhawan, S. Majumdar, E. Rastorgueva, Z. Chen, V. Lavrukhin, J. Balam, and B. Ginsburg, "Less is more: Accurate speech recognition & translation without web-scale data," in *Proc. Interspeech*, 2024, pp. 3964–3968.
- [42] J. S. Garofolo, L. F. Lamel, W. M. Fisher, J. G. Fiscus, D. S. Pallett, N. L. Dahlgren, and V. Zue, "TIMIT acoustic-phonetic continuous speech corpus," Linguistic Data Consortium, Philadelphia, LDC93S1, 1993.
- [43] M. A. Pitt, K. Johnson, E. Hume, S. Kiesling, and W. Raymond, "The Buckeye corpus of conversational speech: Labeling conventions and a test of transcriber reliability," *Speech Communication*, vol. 45, no. 1, pp. 89–95, 2005.
- [44] A. Shrikumar, P. Greenside, and A. Kundaje, "Learning important features through propagating activation differences," in *Proc. ICML*, ser. Proceedings of Machine Learning Research, D. Precup and Y. W. Teh, Eds., vol. 70. PMLR, Aug. 2017, pp. 3145–3153. [Online]. Available: <https://proceedings.mlr.press/v70/shrikumar17a.html>
- [45] M. Ancona, E. Ceolini, C. Öztireli, and M. Gross, "Towards better understanding of gradient-based attribution methods for deep neural networks," in *Proc. ICLR*, 2018. [Online]. Available: <https://openreview.net/forum?id=Sy21R9JAW>
- [46] D. Smilkov, N. Thorat, B. Kim, F. Viégas, and M. Wattenberg, "SmoothGrad: removing noise by adding noise," arXiv:1706.03825, 2017.
- [47] J. Adebayo, J. Gilmer, M. Muelly, I. Goodfellow, M. Hardt, and B. Kim, "Sanity checks for saliency maps," in *Proc. NeurIPS*, S. Bengio, H. Wallach, H. Larochelle, K. Grauman, N. Cesa-Bianchi, and R. Garnett, Eds., vol. 31. Curran Associates, Inc., 2018. [Online]. Available: https://proceedings.neurips.cc/paper_files/paper/2018/file/294a8ed24b1ad22ec2e7efea049b8737-Paper.pdf
- [48] M. Sundararajan, A. Taly, and Q. Yan, "Axiomatic attribution for deep networks," in *Proc. ICML*, ser. Proceedings of Machine Learning Research, D. Precup and Y. W. Teh, Eds., vol. 70. PMLR, Aug. 2017, pp. 3319–3328. [Online]. Available: <https://proceedings.mlr.press/v70/sundararajan17a.html>
- [49] G. Erion, J. D. Janizek, P. Sturmfels, S. M. Lundberg, and S.-I. Lee, "Improving performance of deep learning models with axiomatic attribution priors and expected gradients," *Nature Machine Intelligence*, vol. 3, no. 7, pp. 620–631, Jul. 2021.